Models of ionospheric VLF absorption of powerful ground based transmitters

M. B. Cohen,[1] N. G. Lehtinen,[1] and U. S. Inan[1,2]

Received 5 November 2012; accepted 16 November 2012; published 29 December 2012.

[1] Ground based Very Low Frequency (VLF, 3–30 kHz) radio transmitters play a role in precipitation of energetic Van Allen electrons. Initial analyses of the contribution of VLF transmitters to radiation belt losses were based on early models of trans-ionospheric propagation known as the Helliwell absorption curves, but some recent studies have found that the model overestimates (by 20–100 dB) the VLF energy reaching the magnetosphere. It was subsequently suggested that conversion of wave energy into electrostatic modes may be responsible for the error. We utilize a newly available extensive record of VLF transmitter energy reaching the magnetosphere, taken from the DEMETER satellite, and perform a direct comparison with a sophisticated full wave model of trans-ionospheric propagation. Although the model does not include the effect of ionospheric irregularities, it correctly predicts the average total power injected into the magnetosphere within several dB. The results, particularly at nighttime, appear to be robust against the variability of the ionospheric electron density. We conclude that the global effect of irregularity scattering on whistler mode conversion to quasi-electrostatic may be no larger than 6 dB. **Citation:** Cohen, M. B., N. G. Lehtinen, and U. S. Inan (2012), Models of ionospheric VLF absorption of powerful ground based transmitters, *Geophys. Res. Lett.*, *39*, L24101, doi:10.1029/2012GL054437.

1. Introduction

[2] The near-Earth space environment is filled with energetic particles which threaten orbiting astronauts and satellite. The solar wind interaction with the magnetosphere injects particles into the magnetosphere which are subsequently accelerated to relativistic energies (>1 MeV). There exist two radiation belts, an inner belt between L of 1.2–3, and an outer belt between L of 4–6. The region between them is known as the slot region, and is typically depleted during quiet times, filling temporarily during geomagnetic storms. Satellites launched into orbit, particularly during solar maximum, must be shielded (adding weight and cost), or be at risk for degradation and failure.

[3] The loss processes of energetic electrons are not fully understood. In the outer belt, the dominant processes are believed to include chorus waves, plasmaspheric hiss, lightning-generated whistlers, and radial diffusion [*Thorne*, 2010]. The steadier inner radiation belt may also be influenced by manmade waves emitted by a set of Very Low Frequency (VLF, 3–30 kHz) radio wave transmitters present at mid-latitudes. VLF radio waves are nominally for global communications or ionospheric remote sensing, due to their efficient propagation in the Earth-ionosphere waveguide.

[4] Coherent signals from VLF transmitters are known to interact with radiation belt electrons [*Helliwell*, 1965, p. 279], as have ELF waves generated by the Siple Station transmitter [*Helliwell and Katsufrakis*, 1974] and the HAARP facility in Alaska [*Gołkowski et al.*, 2008]. Efforts to quantify the total role of VLF transmitters were made by *Inan et al.* [1984], and then expanded by *Abel and Thorne* [1998], which found that transmitters play a significant role in determining radiation belt lifetimes below L ~ 2.5, based on data from the 'Starfish' experiment.

[5] The calculations in *Abel and Thorne* [1998] were based on an early model of trans-ionospheric propagation to estimate the power reaching the magnetosphere, known as the 'Helliwell absorption curves' [*Helliwell*, 1965, p. 71]. *Starks et al.* [2008] compared the curves with individual satellite passes and find that the model overestimates the magnetic field by at >20 dB during nighttime, and 10 dB during daytime, in mid-latitudes. *Tao et al.* [2010] note that the ionospheric electron density profile assumed by *Helliwell* [1965, p. 71] was different from both the International Reference Ionosphere (IRI) and from rocket data. If a more realistic profile is used, the overestimation is larger (60–100 dB).

[6] The most prominent theory for explaining this overestimation centers around scattering of the VLF transmitter signal off irregularities in the ionosphere, and their subsequent conversion into quasi-electrostatic modes with high wave normal angle, which do not propagate efficiently. *Bell et al.* [2011] present DEMETER observations showing a clear impact of VLF heating on the ionosphere observable at 700 km altitude, which are not taken into account in 'smooth ionosphere' models such as in *Helliwell* [1965, p. 71], *Lehtinen and Inan* [2009] and *Tao et al.* [2010]. Theoretical calculations can explain 3–6 dB of loss in the F-region from irregularities [*Foust et al.*, 2010]. *Shao et al.* [2012] account for irregularities generated by the nonlinear VLF transmitter heating and calculate 9–15 dB of loss in the D and E regions.

[7] *Cohen and Inan* [2012] present an extensive set of VLF transmitter measurements based on six years of compiled observations from the DEMETER satellite (680 km altitude) using survey mode data that include one electric and one magnetic field horizontal component. With this large database, the full radiation pattern is observed, both day and night, and the total power injected into the

[1]Department of Electrical Engineering, Stanford University, Stanford, California, USA.
[2]Department of Electrical Engineering, Koc University, Sariyer-Istanbul, Turkey.

Corresponding author: M. B. Cohen, 350 Serra Mall Rm. 356, Stanford, CA 94305, USA. (mcohen@stanford.edu)

0094-8276/12/2012GL054437

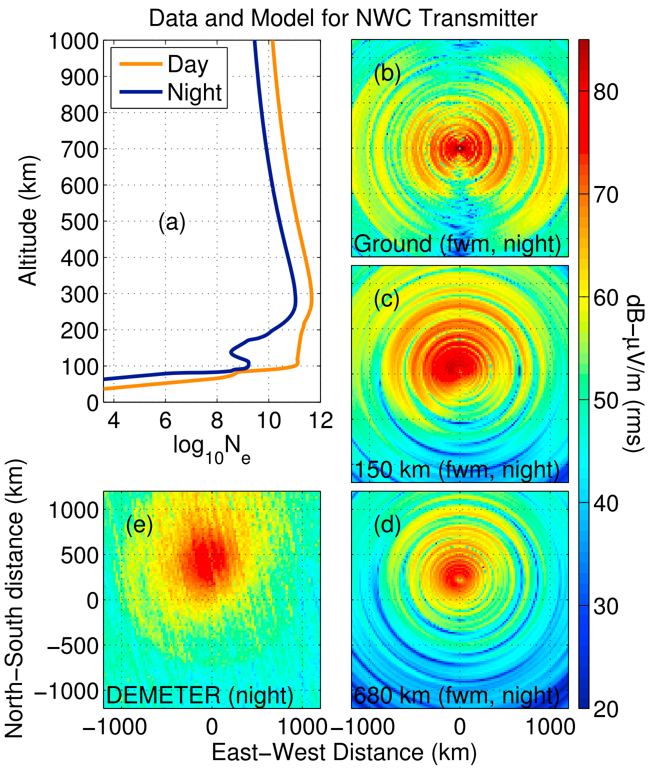

Figure 1. Comparison of data and modeling for the NWC transmitter (1 MW, 19.8 kHz). (a) The ionospheric electron density profile used, taken from the IRI. The calculated magnetic field (one horizontal component) (b) on the ground, (c) at 150 km altitude, and (d) at 680 km altitude, with the transmitter located at the origin. (e) The observed radiation pattern from DEMETER, taken from *Cohen and Inan* [2012].

magnetosphere summed, giving much more detail than individual satellite passes provide. In this paper, we provide an initial comparison of these measurements with a full wave model described by *Lehtinen and Inan* [2008] and *Lehtinen and Inan* [2009], and to the Helliwell absorption curves.

2. Modeling Results

[8] *Lehtinen and Inan* [2008] and *Lehtinen and Inan* [2009] describe the full wave model of VLF transmitter propagation. We assume a flat Earth with $\sigma = 10^{-4}$ S/m, and horizontally stratified slabs. The model calculates the reflection coefficient at each slab boundary and the modal solutions at specified locations either in or below the ionosphere. The method is similar to many previous analytical methods (summarized by *Budden* [1985, chapter 18]) but utilizes a new calculation method to eliminate the numerical 'swamping' problem that plagued earlier efforts.

[9] Figure 1 shows the inputs and outputs of the model, applied to the NWC transmitter in Australia (21.816°S, 114.166°E), radiating 1 MW at 19.8 kHz. The geomagnetic field is taken from the IGRF model. Figure 1a shows the ionospheric electron density, taken from the IRI model for both daytime (02:24 UT on 21-Jun-2007) and nighttime (14:24 UT on 21-Dec-2007). The collision frequency includes electron-neutral and electron-ion collisions as in *Swamy* [1992], as used by *Lehtinen and Inan* [2009]. Figures 1b–1e show the results from the nighttime comparison. The source is assumed to be a vertical current dipole 100 m above the ground. Figures 1a and 1e show the calculated radiation pattern from NWC (one component of the horizontal electric field, RMS amplitude) on the ground (Figure 1b), 150 km altitude (Figure 1c), and 680 km altitude (Figure 1d), over a 2500 × 2500 km area around the transmitter.

[10] The ground signal is dominated by propagation in the Earth-ionosphere waveguide, with a modal interference pattern that manifests as concentric rings around the transmitter. Most of the absorption of VLF waves occurs in the *D* and *E* regions (i.e. below 150 km), after which point the wave propagates mostly along magnetic field lines, so that the ground model interference pattern is still evident, resembling the upward mapping of the ground interference pattern observed by *Parrot et al.* [2008]. The energy from the transmitter is strongest in a ~300 km radius around a point centered ~250 km to the north of the transmitter, due to the bending of the VLF energy along the magnetic field.

[11] Figure 1e shows the observations of the electric field (RMS amplitude) from the six-year DEMETER data, as shown in *Cohen and Inan* [2012], excluding one long period in 2007 when NWC was off for maintenance. The data are binned into 25 km pixels and plotted over the same spatial range and colorscale for direct comparison.

[12] Figure 2 shows the observed and modeled electric field values for 10 VLF transmitters at nighttime. Each horizontal set of three panels corresponds to one transmitter, whose call signs and frequencies are labeled at the top of the first two panels. The first of the three panels show the observed electric field data from DEMETER averaged over its lifetime [*Cohen and Inan*, 2012] using the calibrated color scale in the top right edge. The middle panel shows the calculated electric field data from the full wave model, using the same color scale. The third panel show the difference (in dB) between the modeled and observed data, using the dimensionless color scale in the bottom right edge. High ratios (red) indicate that the model results overestimate the field strength, while low ratios (blue) means the model results underestimate the field strength, and light colors mean the model and data are fairly close.

[13] The radiated powers taken as input to simulate the fields at 700 km are not known exactly but are estimated (at worst a couple dB error) based either on near field measurements by the transmitter operators, or from comparisons of the fields on the ground with validated subionospheric propagation models such as Long Wave Propagation Capability [*Ferguson*, 1988]. The three transmitters at 14.88 kHz form the Russian 'Alpha' network, a ground based predecessor to GPS.

[14] It is difficult to directly compare the spatial pattern of the averaged radiation to a single model run. As seen in Figures 2 and 3, the calculated pattern has finer detail in the interference pattern. This difference results from the variability of the ionosphere from day to day. The spacing of the concentric ring interference pattern is largely set by the reflection height of VLF waves in the Earth-ionosphere waveguide, so that an averaged pattern over six years

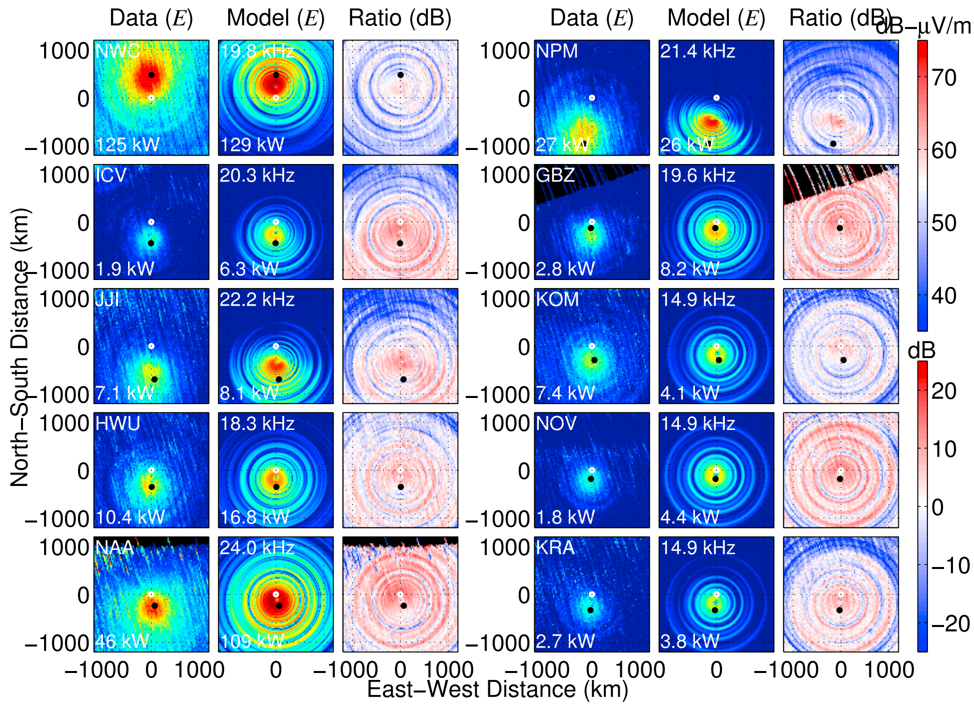

Figure 2. Side by side comparisons of the observed and modeled VLF transmitter signals for each of 10 VLF transmitters (nighttime).

contains an amalgamation of observations with different ionospheres, which smooths the averaged pattern.

[15] The model correctly predicts the location of the energy emerging from the ionosphere, which is largely a function of the geomagnetic field direction. On each of the plots, a black dot indicates the location of the magnetic field line traced from 80 km above the transmitter, to the altitude 680 km, and the white dot is the location directly above the transmitter. On the other hand, the energy released by lower latitude transmitters such as NPM emerges hundreds of km equator-ward from the transmitter. The wave energy exits the ionosphere close to the geomagnetic field direction,

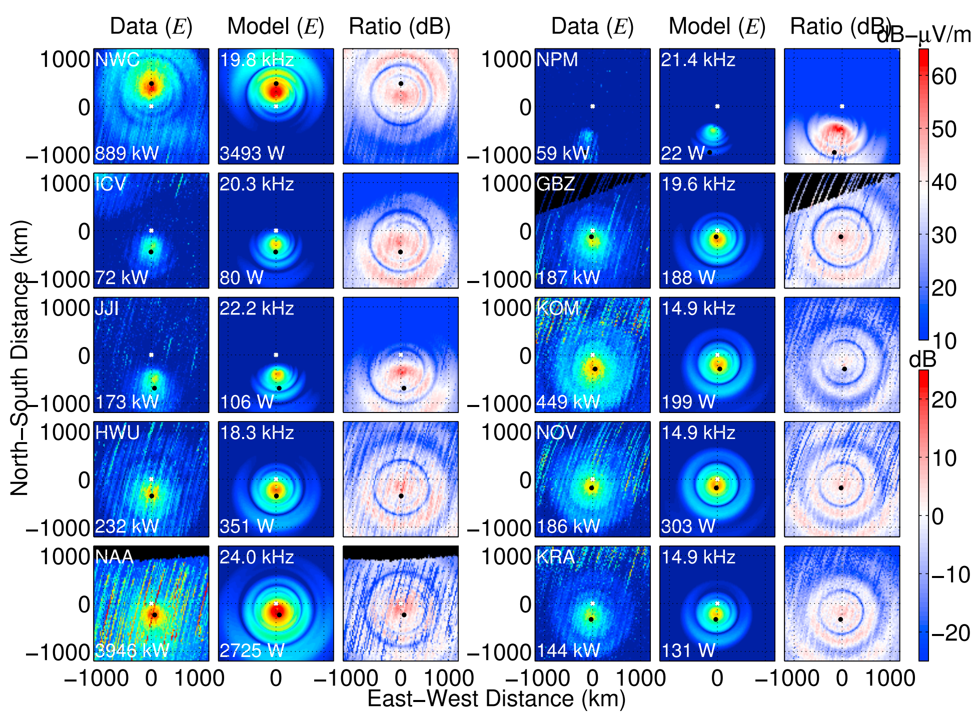

Figure 3. Same as Figure 2 but for daytime.

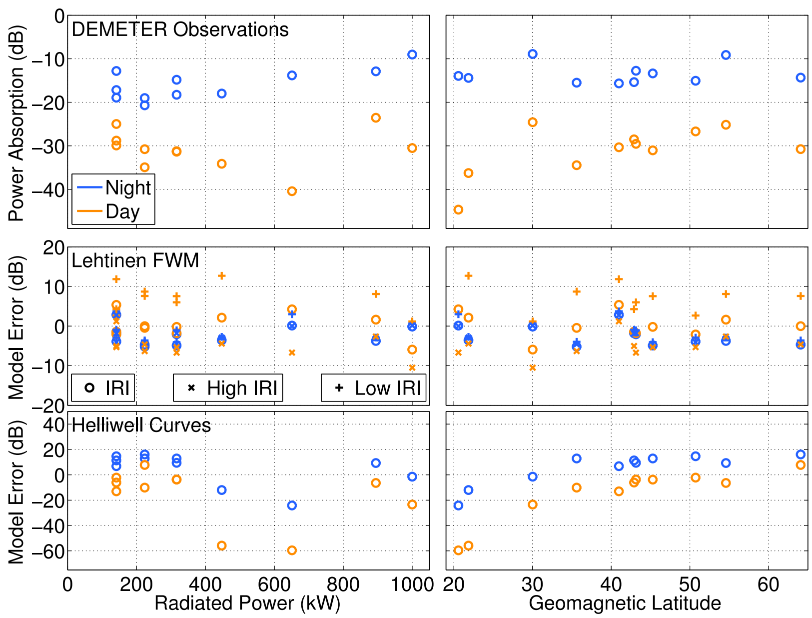

Figure 4. Comparison of trans-ionospheric absorption models to observations. (top) The DEMETER-inferred absorption as a function of (left) radiated power of the transmitter and (right) geomagnetic latitude. (middle) The error of full wave model calculations, with positive values indicating an overestimation of the total power by the model. Values using the 'true' IRI, as well as scaled versions with both higher and lower density are indicated. (bottom) the error of the Helliwell absorption curves.

nearly parallel along the field line. Figure 3 shows the same comparison for daytime cases, and all the results are very similar. The same figures for magnetic field are included as auxiliary material.[1]

[16] One notable shortcoming is apparent for the NPM comparison. The azimuthal distribution of the emerging power is beamed southward in the observed data more than in the model. This result is likely due to the horizontal stratification of the model, which takes a single value of the geomagnetic field in each plane. NPM is close enough to the equator that the power radiating southward encounters a rapidly changing geomagnetic field.

[17] *Cohen and Inan* [2012] present calculations of the total power injected into space from each transmitter, using both the electric and magnetic field recordings from the DEMETER satellite survey mode. Electromagnetic waves propagating into the magnetosphere in this frequency range are dominated by the whistler mode, a right hand circularly polarized wave, allowing approximation of the Poynting Flux from $\vec{S}_{av} = \frac{1}{2}\left|\vec{E} \times \vec{B}/\mu_0\right|$ since propagation is nearly (within 10°) parallel to the geomagnetic field. The total power is found by integrating that flux over the region encompassing the energy from the transmitter, as described by *Cohen and Inan* [2012], and is calculated in the same manner for the model results.

[18] The total power of both the observed and calculated radiation patterns into the ionosphere are labeled in the panels in Figures 2 and 3. For nighttime calculations, the model errors range from a 5.2 dB overestimation (ICV) to a 2.6 dB underestimation (KOM). For daytime calculations, the model errors range from a 5.9 dB overestimation of the total power at 700 km (NWC) to a 4.2 dB underestimation (NPM).

3. Discussion

[19] The ionospheric variability presents some uncertainty in our results. The collision frequency choice may impact the trans-ionospheric propagation by 0–3 dB, as seen in Figure 2c of *Lehtinen and Inan* [2009]. However, the choice of electron density is very important [*Tao et al.*, 2010].

[20] The IRI is known to be less accurate for the *D*-region, particularly at nighttime, although the ionospheric absorption of VLF waves may be dominated by the *D* region. *Tao et al.* [2010, Figure 6] addressed this uncertainty by analyzing a large number of rocket passes through the ionosphere, and finding a variability of nearly 1–2 orders of magnitude for the nighttime electron density in the *D* region, and 0.5–1 order of magnitude for the daytime electron density.

[21] To rule out a systematic error, we repeat the simulations with scaled versions of the IRI model. The model calculations are repeated with the electron density doubled and halved for daytime, multiplied by 5 and by 1/5 for nighttime. This technique injects a similar variability into the model calculations as may be in the IRI, and bounds our theoretical calculations. The nighttime power absorption calculation was altered by ±1 dB or less in all cases, while the daytime power absorption calculations changed by ±5–10 dB. *Tao et al.* [2010] found that correcting the electron density in the Helliwell absorption curve using rocket pass based data reduced the predicted absorption by 4–8 dB for 20 kHz at night, and 20–30 dB at daytime, in agreement with the conclusion here that the electron density variations in the daytime have a larger effect.

[22] Figure 4 shows a comparison between observations and modeling. The top row shows the total DEMETER-

[1]Auxiliary materials are available in the HTML. doi:10.1029/2012GL054437.

derived absorption, defined as the ratio of the power at 700 km to the radiated power on the ground. The left panel shows the absorption as a function of the radiated power, the right panel as a function of geomagnetic latitude (defined as $\arccos\left(\sqrt{\frac{1}{L}}\right)$ with respect to the L-shell value taken from the IGRF model for 80 km above the transmitter). The lower two rows show the error between the model and observations for the full wave model described by *Lehtinen and Inan* [2008] (Figure 4, middle), and the 20 kHz Helliwell absorption curves [*Helliwell*, 1965, p. 71] (Figure 4, bottom). Positive values indicate that the model overestimates the power reaching the satellite.

[23] For the Lehtinen model, the calculated and observed powers for each transmitter are within 6 dB for each transmitter and both daytime and nighttime with the correct IRI. Even when including the large uncertainty in the ionospheric electron density, the model calculations are within 6 dB of the observed values for nighttime, and within 12 dB for daytime, with one exception (NPM). It is possible that the magnetic field strength is correctly estimated by the model near the transmitter but is incorrect at large distances.

[24] *Lehtinen and Inan* [2009] looked at a small number of satellite passes and found that the model overestimates the field by ~10 dB. This result was in part due to the differing method of model-data comparison, and in part because *Lehtinen and Inan* [2009] only carried the calculations out to 110 km altitude, and then projected the power flux to 700 km. In this present work we extended the full wave calculations all the way to 680 km.

[25] At low latitudes, the Helliwell curves underestimate the absorbed power by as much as 20–60 dB due to its known shortcoming for nearly horizontal geomagnetic field lines. At mid latitudes, the Helliwell curves appear to overestimate the nighttime power by ~10–15 dB, and underestimate the daytime power by ~10 dB. This indicates slightly closer agreement than found by *Starks et al.* [2008].

[26] The model error does not appear to be a strong function of transmitter power. The conversion from whistler mode to quasi-electrostatic modes *Shao et al.* [2012] relies at least in part on coherent transmitter heating for the generation of irregularities, leading to nonlinear transionospheric absorption. However, our results appear to suggest that the transionospheric absorption is linear at least up to 1 MW. We conclude that existing ‘smooth’ full wave models of transionospheric absorption correctly predict the total power injected into the magnetosphere from VLF transmitters within 6 dB, especially at nighttime.

[27] Future work will compare the spatial pattern of the predicted and observed power and fields, to more precisely establish the global role (if any) of ionospheric irregularities. There is also a need for a set of absorption curves to replace those of *Helliwell* [1965, p. 71].

[28] **Acknowledgments.** This work has been supported by AFRL award FA9453-11-C-0011 to Stanford University. We thank Michael Starks, Kevin Graf, Peder Hansen, and Dave Lauben for helpful discussions. We thank the DEMETER team, including Michel Parrot and Jean Jacques Berthelier for making the IMSC and ICE data available.

[29] The Editor thanks one anonymous reviewer for assistance in evaluating this paper.

References

Abel, B., and R. M. Thorne (1998), Electron scattering loss in Earth's inner magnetosphere: 1. Dominant physical processes, *J. Geophys. Res.*, *103*(A2), 2385–2396.

Bell, T. F., K. L. Graf, U. S. Inan, D. Piddyachiy, and M. Parrot (2011), DEMETER observations of ionospheric heating by powerful VLF transmitters, *Geophys. Res. Lett.*, *38*, L11103, doi:10.1029/2011GL047503.

Budden, K. G. (1985), *The Propagation of Radio Waves: The Theory of Radio Waves of Low Power in the Ionosphere and Magnetosphere*, Cambridge Univ. Press, Cambridge, U. K.

Cohen, M. B., and U. S. Inan (2012), Terrestrial VLF transmitter injection into the magnetosphere, *J. Geophys. Res.*, *117*, A08310, doi:10.1029/2012JA017992.

Ferguson, J. A. (1988), Computer programs for assessment of long-wavelength radio communications, version 2.0, *Tech. Rep. Doc. 3030*, Space and Nav. Warfare Syst. Command, San Diego, Calif.

Foust, F. R., U. S. Inan, T. F. Bell, and Lehtinen (2010), Quasi-electrostatic whistler mode wave excitation by linear scattering of EM whistler mode waves from magnetic field-aligned density irregularities, *J. Geophys. Res.*, *115*, A11310, doi:10.1029/2010JA015850.

Gołkowski, M., U. S. Inan, A. R. Gibby, and M. B. Cohen (2008), Magnetospheric amplification and emission triggering by ELF/VLF waves injected by the 3.6 MW HAARP ionospheric heater, *J. Geophys. Res.*, *113*, A10201, doi:10.1029/2008JA013157.

Helliwell, R. A. (1965), *Whistlers and Related Ionospheric Phenomena*, Dover, New York.

Helliwell, R. A., and J. P. Katsufrakis (1974), VLF wave injection into the magnetosphere from Siple Station, Antarctica, *J. Geophys. Res.*, *79*(16), 2511–2518.

Inan, U. S., H. C. Chang, and R. A. Helliwell (1984), Electron precipitation zones around major ground-based VLF signal sources, *J. Geophys. Res.*, *89*(A5), 2891–2906.

Lehtinen, N. G., and U. S. Inan (2008), Radiation of ELF/VLF waves by harmonically varying currents into a stratified ionosphere with application to radiation by a modulated electrojet, *J. Geophys. Res.*, *113*, A06301, doi:10.1029/2007JA012911.

Lehtinen, N. G., and U. S. Inan (2009), Full-wave modeling of transionospheric propagation of VLF waves, *Geophys. Res. Lett.*, *36*, L03104, doi:10.1029/2008GL036535.

Parrot, M., U. S. Inan, and N. G. Lehtinen (2008), V-shaped VLF streaks recorded on DEMETER above powerful thunderstorms, *J. Geophys. Res.*, *113*, A10310, doi:10.1029/2008JA013336.

Shao, X., B. Eliasson, A. S. Sharma, G. Milikh, and K. Papadopoulos (2012), Attenuation of whistler waves through conversion to lower hybrid waves in the low-altitude ionosphere, *J. Geophys. Res.*, *117*, A04311, doi:10.1029/2011JA017339.

Starks, M. J., R. A. Quinn, G. P. Ginet, J. M. Albert, G. S. Sales, B. W. Reinisch, and P. Song (2008), Illumination of the plasmasphere by terrestrial very low frequency transmitters: Model validation, *J. Geophys. Res.*, *113*, A09320, doi:10.1029/2008JA013112.

Swamy, A. C. (1992), Equatorial electro-jet parameters and the relevance of electromagnetic drafts (EMD) over Thumba, *Astrophys. Space Sci.*, *191*, 203–211.

Tao, X., J. Bortnik, and M. Friedrich (2010), Variance of transionospheric VLF wave power absorption, *J. Geophys. Res.*, *115*, A07303, doi:10.1029/2009JA015115.

Thorne, R. M. (2010), Radiation belt dynamics: The importance of wave-particle interactions, *Geophys. Res. Lett.*, *37*, L22107, doi:10.1029/2010GL044990.